ACS Sustainable Chemistry & Engineering

pubs.acs.org/journal/ascecg

Research Article

Quantification of Phenolic Hydroxyl Groups in Lignin via ^{19}F NMR Spectroscopy

Jacob K. Kenny, J. Will Medlin, and Gregg T. Beckham*

Cite This: *ACS Sustainable Chem. Eng.* 2023, 11, 5644−5655

Read Online

ACCESS | Metrics & More | Article Recommendations | Supporting Information

ABSTRACT: Phenolic moieties strongly influence lignin reactivity and physical properties, and thus accurate quantification of phenolic groups in lignin is a critical analytical chemistry need. Today, ^{31}P nuclear magnetic resonance (NMR) spectroscopy is widely considered the standard method to this end, but this approach uses a hazardous and expensive derivatization agent, and the NMR spectroscopy experiments are time consuming due to long relaxation times. Here, we report a complementary method that enables accurate identification and quantification of phenolic groups in lignin samples using pentafluoropyridine (PFP) as a derivatizing reagent followed by ^{19}F NMR spectroscopy. Using dimethyl sulfoxide as a solvent in the presence of K_2CO_3, phenolic hydroxyl groups in lignin model compounds were fully converted to the corresponding tetrafluoropyridyl-ether products within 1 min. PFP exhibits high selectivity for the reaction with phenolic hydroxyl groups relative to aliphatic alcohols, and we show that side reactions with carboxylic acids, if present, can be avoided through the addition of 40% water to the reaction solvent. The PFP ^{19}F method achieved similar results compared to ^{31}P NMR spectroscopy when applied to reductive catalytic fractionation oil from poplar, softwood kraft lignin, and corn stover milled wood lignin, thereby offering a safe and cost-effective method for phenolic measurements in lignin.

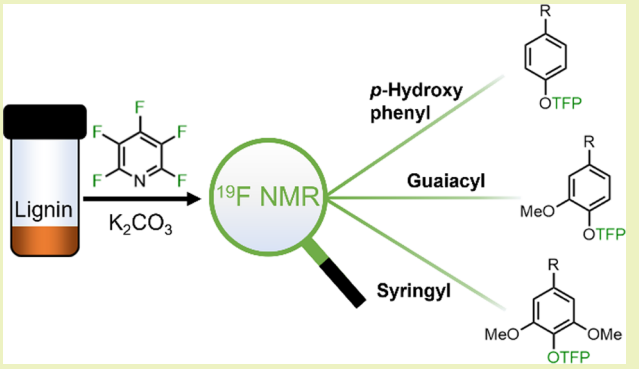

KEYWORDS: *pentafluoropyridine, fluorine, analytical chemistry, biomass conversion, ^{31}P NMR*

INTRODUCTION

Lignin is a complex plant heteropolymer formed from the radical coupling reactions of monolignols that include *p*-coumaryl, coniferyl, and sinapyl alcohols, producing the *p*-hydroxyphenyl (H), guaiacyl (G), and syringyl (S) aromatic units in the polymer linked via C−O (e.g., *β*-O-4 and 4-O-5) and C−C (e.g., *β*-*β*, *β*-1, and 5-5) bonds.[1] In recent years, additional monolignols have been reported that further expand the chemical diversity in this plant biopolymer.[2] Lignin has been widely recognized as a source of renewable aromatic compounds, and process modeling and analysis to this end have demonstrated that lignin valorization to fuels, chemicals, and materials is essential to the viability of lignocellulosic biorefining.[3−7] To date, many promising approaches to extract and valorize lignin from plants have been investigated, many of which induce chemical changes in the polymer. The resulting distribution of functional groups in lignin-derived products, particularly phenolic hydroxyl groups, governs both reactivity and material properties.[3,8−10] Thus, accurate identification and quantification of these phenolic hydroxyl groups are important for lignin valorization pursuits.

Various methods for characterizing phenolic groups in lignin have been reported, including infrared spectroscopy, UV−vis spectroscopy, and ^{1}H nuclear magnetic resonance (NMR) spectroscopy. However, they have not seen widespread use due to insufficient ability to resolve and quantify more detailed structural features, such as the substitution pattern *ortho* to the phenol.[11−14] A ^{19}F NMR method utilizing fluorobenzylation was reported by Barrelle and others, but isolation of the derivatized lignin was required prior to analysis; moreover, a significant overlap between the derivatization agent and phenolic groups in the ^{19}F spectrum was observed.[15−17] Quantitative ^{13}C NMR spectroscopy is rich in structural information, and reports combining analysis of acetylated and underivatized samples can quantify a vast array of structural features, which are useful for sample fingerprinting.[18,19] Nevertheless, ^{13}C NMR spectroscopy for lignin suffers drawbacks due to large sample amounts required and/or long NMR experiment acquisition times for spectrometers not equipped with a cryoprobe, complex spectra, and overlap between phenolic hydroxyl group resonances.[11,20]

Received: January 7, 2023
Revised: March 2, 2023
Published: March 28, 2023

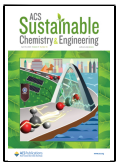

One of the most widely implemented methods for quantifying phenolic groups in lignin is phosphitylation followed by ^{31}P NMR spectroscopy analysis.[21] Originally used to characterize coal condensates,[22,23] the method was adapted for lignin characterization by Argyropoulos *et al.* and has since been extensively applied on a variety of lignins.[24−26] Briefly, a derivatizing agent, commonly 2-chloro-4,4,5,5-tetramethyl-1,3,2-dioxaphospholane (TMDP), is combined with the lignin sample dissolved in pyridine/deuterated chloroform. From a 1D ^{31}P NMR experiment, distinct resonances are obtained for aliphatic alcohols, carboxylic acids, and various phenolics (5-substituted, G, and H) that are integrated relative to an internal standard. The advantages of the ^{31}P NMR method include the organic solvent mixture capable of dissolving a variety of lignins, commercially available reagents, and a straightforward procedure and NMR experiment. However, the method also suffers from several drawbacks. Importantly, the phosphitylation reagent is hazardous, with the potential for serious skin and eye damage (GHS 1B skin corrosion, category 1 serious eye damage) upon exposure. It is also expensive ($217/g from Sigma-Aldrich at the time of writing) and degrades if exposed to moisture. Furthermore, NMR experimental times of ∼1 h per sample are required due to high spin−lattice relaxation values (T_1) of the phosphorus nuclei. When coupled with the limited stability of the derivatized samples, the throughput for ^{31}P NMR measurements is limited.[27]

Recently, pentafluoropyridine (PFP) was shown to be an effective phenol protecting group by selectively reacting at its 4-position to form the corresponding tetrafluoropyridyl (TFP) ether.[28] In this work, we demonstrate that PFP can fully react with phenolic groups in lignin to form the corresponding TFP ethers. These TFP ethers exhibit distinct chemical shifts in a ^{19}F NMR spectrum based on their *ortho*-substitution. The effects of reaction time, solvent, and ring substitution pattern on the rate of reaction were investigated, and the optimum system was found to be 40% H_2O/DMSO with a reaction time of 5 min. Given these results, the method potentially offers a safer (GHS category 4 acute toxicity for PFP) and cheaper ($6.04/g for PFP on Sigma-Aldrich at the time of writing) alternative to ^{31}P NMR to quantify phenolic content in lignin samples.

MATERIALS AND METHODS

As described below, we tested the use of ^{19}F NMR spectroscopy with multiple lignin substrates, including lignin oil from reductive catalytic fractionation (RCF) of poplar and corn stover milled wood lignin (MWL). We describe the preparation, ^{31}P derivatization, and NMR measurements for these samples fully in the Supporting Information (SI).

Materials. We purchased multiple chemicals from Sigma-Aldrich, including PFP, dimethyl sulfoxide (DMSO), acetone, 4,4-difluorobenzophenone, potassium carbonate (K_2CO_3), 4-propylguaiacol, 4-propylphenol, syringol, guaiacol, phenol, vanillin, syringaldehyde, *p*-hydroxybenzoic acid, vanillic acid, syringic acid, vanillin, syringaldehyde, vanillyl alcohol, syringyl alcohol, 3,4-dimethoxybenzyl alcohol, homovanillyl alcohol, 2-(3,4-dimethoxyphenyl)-ethanol, 3-(3,4-dimethoxyphenyl)-1-propanol, 4-hydroxybenzyl alcohol, 4-methoxybenzyl alcohol, 2-(4-hydroxyphenyl)-ethanol, 2-(4-methoxyphenyl)-ethanol, chromium(III) acetylacetonate ($Cr(acac)_3$), softwood alkali kraft lignin (SWKL), ruthenium on carbon (Ru/C, 5 wt % metal), methanol, and d_6-acetone. Guaiacylglycerol-beta-guaiacyl ether (GGE) and 4-propanolguaiacol were purchased from TCI, and 1-(3,4-dimethoxyphenyl)-2-(2-methoxyphenoxy)propane-1,3-diol (VGE) ether was purchased from Matrix Scientific. 4-Propylsyringol was synthesized from 4-allyl-2,6-dimethoxyphenol (Sigma-Aldrich).[29] The 5-5 GG model compound was produced according to previously published methods.[30]

Model Compound and Lignin Derivatization. The substrate (either lignin or a model compound, typically between 20 and 40 mg) was loaded into a 10 mL vial with a stir bar. K_2CO_3 (4 molar equivalents based on the phenol content, unless otherwise specified) was added. The internal standard (4,4-difluorobenzophenone) was then added, and the mass was recorded. The solvent was then added via a volumetric pipette. PFP (4 molar equivalents based on the phenol content, unless otherwise specified) was then added with a volumetric pipette to each vial. The vials were briefly (∼3 s) shaken by hand to mix all the components and put onto a stir plate at 800 rpm, at which point the timer was started. Depolymerized lignins such as organosolv or kraft lignins typically contain higher amounts of phenolic groups compared to native lignins but vary widely depending on the process and biomass used.[11,31] For lignin samples, a phenol content of 4 mmol/g was assumed for the calculation of the required K_2CO_3 and PFP. After the desired reaction time, a sample was taken by filtering the reaction mixture through a 0.2 μm PTFE syringe filter. For reactions in pure solvent, this was done directly from the reaction mixture and was repeated over the course of the reaction to obtain time course measurements. For reactions in H_2O/DMSO, 2 mL of acetone was added to each vial prior to sampling to resolubilize the lignin and internal standard, and the vials were shaken. For model compounds, poplar RCF oil, and corn stover MWL, resolubilization was almost instantaneous. However, for kraft lignin, the vials needed to be shaken for approximately 1 min before the sample fully was dissolved. Subsequently, 0.3 mL of the filtered sample was combined with 0.3 mL of acetone-d_6/$Cr(acac)_3$ (2 mg/mL initial concentration of the d_6-acetone solution, for a final sample $Cr(acac)_3$ concentration of 1 mg/mL).

^{19}F NMR Experiments. A 1D ^{19}F NMR experiment with inverse gating was acquired on a Bruker Avance 300 MHz instrument with a delay of 6 s, 64 scans, and a sweep width of 242 ppm. Processing was performed using TopSpin 3.7. The file was apodized with an exponential line broadening of 2.0 Hz. The internal standard peak was located and set to −108.4 ppm for reactions in acetone, −106.4 ppm for reactions in DMSO, or −107.4 ppm for reactions in 40% H_2O/DMSO. The internal standard peak was made as symmetrical as possible through first-order phasing. Then, the PFP peak at −135 ppm was adjusted to be symmetric with first-order phasing. The baseline was then corrected using a sixth-order Bernstein polynomial fit in the order of ranges −80 through −110, then −110 through −145, and finally −145 through −165 ppm. The MestreNova automatic multipoint baseline correction feature was also found to give satisfactory results. Plots of the NMR spectra were produced using MestreNova 14.1.

RESULTS AND DISCUSSION

Method Development with Phenolic Model Compounds. PFP has been shown to undergo S_NAr reactions with a range of phenolic substrates in the presence of a base.[28,32] In these reactions, the base deprotonates the phenol to form the phenolate ion, which then adds to PFP, followed by elimination of the fluoride ion to form the TFP-ether product (Figure 1A). When a weak base such as K_2CO_3 is used at room temperature, this reaction occurs exclusively at the 4-position of PFP; however, stronger bases and elevated temperatures have been used to enable reactivity at sites *ortho* and *meta* to the nitrogen atom.[33] This reaction produces a stoichiometric amount of HF, but the excess of K_2CO_3 converts the HF to KF or other potassium fluoride species (see the SI for discussion of chemical safety).[34] By including an internal standard (4,4-difluorobenzophenone) in the reaction setup, we envisioned a method where the reaction mixture can simply be filtered after the desired reaction time to yield a solution that can be

https://doi.org/10.1021/acssuschemeng.3c00115
ACS Sustainable Chem. Eng. 2023, 11, 5644−5655

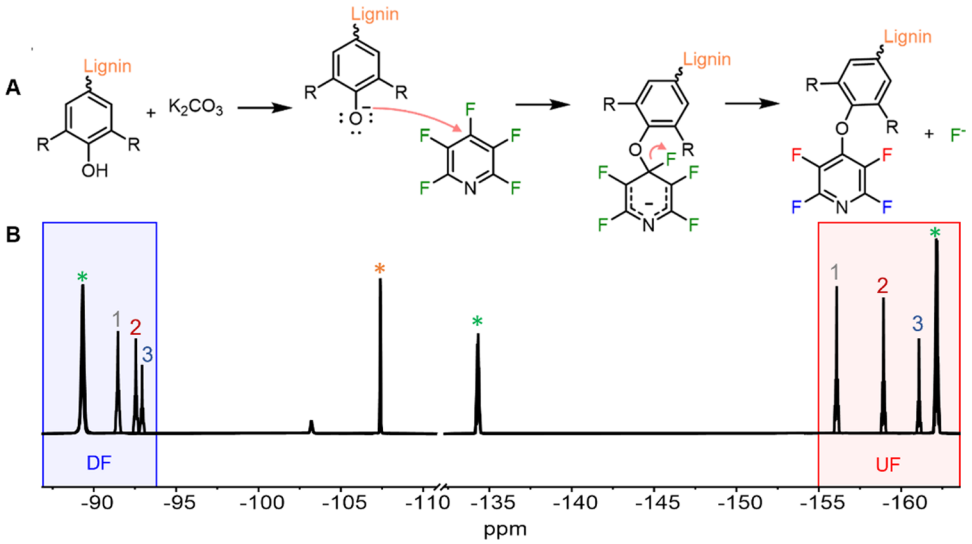

Figure 1. (A) Reaction of PFP with a phenolic compound to form a TFP ether through an S_NAr mechanism. (B) The blue and red fluorine atoms in the TFP product correspond to the ^{19}F NMR resonance regions from −89 to −95 (DF) and −155 to −162 (UF), respectively. Resonances marked with a green asterisk belong to PFP, and the resonance marked with an orange asterisk is for the internal standard, 4,4-difluorobenzophenone. Numbered resonances correspond to 4-propylphenol (1), 4-propylguaiacol (2), and 4-propylsyringol (3) derivatized in 40% H_2O/DMSO.

analyzed via ^{19}F NMR to quantitatively measure phenolic groups.

To explore the viability of the proposed ^{19}F NMR method for identifying and quantifying phenolic groups in lignin, reactions were first performed on model compounds representative of the chemical motifs found in lignin (Table S1). In the proposed method, phenols must react completely to form the corresponding TFP ethers without the formation of side products and in a reasonable amount of time. Furthermore, the ^{19}F NMR resonance must be sensitive to the substitution *ortho* to the ether bond to enable the identification and quantification of different types of phenols. To examine the viability of this approach, experiments were first performed on a series of 4-propyl-substituted monomers, namely, 4-propylphenol, 4-propylguaiacol, and 4-propylsyringol, which mimic the H-, G-, and S-type substitution patterns found in lignin, respectively. Reactions were conducted in 10 mL vials at room temperature with magnetic stir bars. The TFP ether contains two sets of identical fluorine atoms, which give rise to resonances in two distinct regions in the ^{19}F NMR spectra: a downfield (DF) region from −89 to −95 ppm (blue fluorine atoms, blue integration region in Figure 1B) and an upfield (UF) region from −155 to −162 ppm (red fluorine atoms, red integration region in Figure 1B). Conversion of the model compound can be determined by integration of peaks in either region relative to the internal standard.

When reactions were performed in acetone with 4 equiv of PFP and K_2CO_3, full conversion of each of the three 4-propyl-substituted compounds to the desired TFP-ether product was measured within 2 h (Figure 2A), and no side products were observed in the ^{19}F spectra. The rate of reaction followed the order 4-propylphenol (H) ∼ 4-propylguaiacol (G) > 4-propylsyringol (S), presumably due to steric hindrance by the *ortho* methoxy groups in the case of 4-propylsyringol. The ^{19}F NMR resonances of the TFP-ether products were also impacted by the substitution pattern *ortho* to the phenol. In both UF and DF regions, 4-propylphenol exhibited the furthest downfield shift, followed by 4-propylguaiacol, and then 4-propylsyringol. However, the separation between the resonances was larger in the UF region (Figure 1B). Similar dependencies of substitution on the reaction rate and ^{19}F NMR shift were observed for both unsubstituted (phenol, guaiacol, and syringol) and aldehyde-substituted (*p*-hydroxybenzaldehyde, vanillin, and syringaldehyde) model compounds (Figure 2B). Aldehyde reactions were conducted in DMSO due to solubility limitations in acetone, as discussed in further detail below. The stir bar size was also observed to affect the rate of reaction. When a medium stir bar (15 × 6 mm, which is the size used for model compound reactions) was used for the derivatization of syringol, full conversion was observed within 2 h, similar to 4-propylsyringol. However, using a smaller stir bar (13 × 3 mm) extended the time necessary for complete derivatization to approximately 12 h. Further increasing the stir bar size (30 × 8 mm) showed no increase in the reaction rate (Figure S1A,B).

To further investigate factors impacting the reaction rate, the slate of model compounds used was expanded. The G-type model compounds guaiacol, 4-propylguaiacol, and vanillyl alcohol all showed similar yields of the TFP ether after 5 min of reaction time in acetone (Figure 2C). However, when vanillin and acetophenone were used under the same conditions, the reactions exhibited higher conversions at 5 min, with the vanillin reaction being complete. These differences correlate with the relative acidities of the aromatic compounds (guaiacol pK_a = 9.93; 4-propylguaiacol pK_a = 9.85; vanillyl alcohol pK_a = 9.78; vanillin pK_a = 7.36; acetovanillone pK_a = 7.81)[35] and indicate that the population of the phenolate may be governing the observed reaction rates. In general, the phenolic hydroxyl groups on compounds where the α-position is a ketone, ester, or aldehyde are more acidic than those where the α-hydroxyl is still present or has been removed or etherified.[35] A single lignin sample can contain multiple functionalities at the α-positions, and this is expected to impact the observed rate of reaction of different lignin samples accordingly.[20,36,37]

https://doi.org/10.1021/acssuschemeng.3c00115
ACS Sustainable Chem. Eng. 2023, 11, 5644−5655

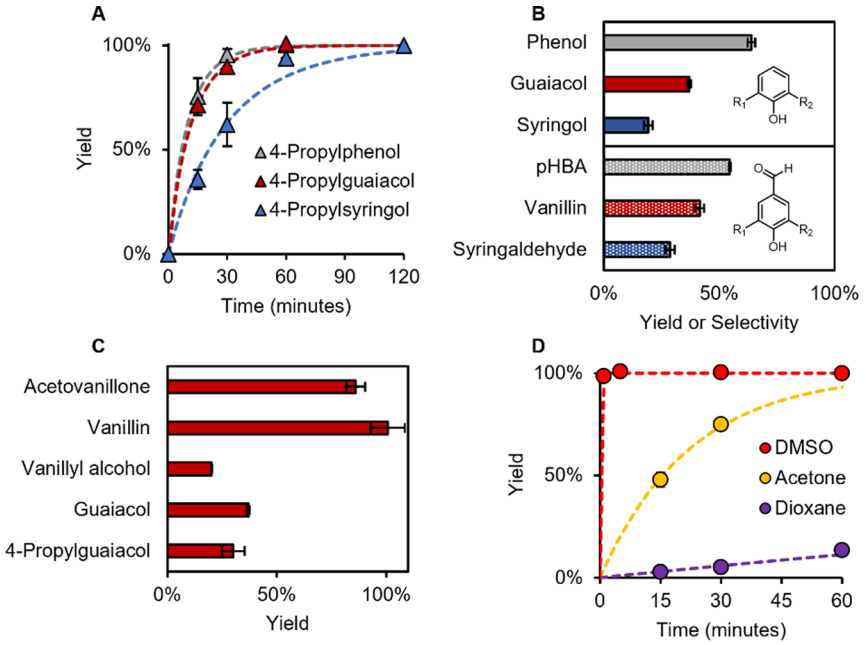

Figure 2. (A) Time course measurement of TFP-ether formation for 4-propylphenol (H), 4-propylguaiacol (G), and 4-propylsyringol (S) in acetone. Conditions: 4 mL of acetone, 4 equiv of K_2CO_3 and PFP, room temperature. (B) Yield of TFP ether for phenol, guaiacol, and syringol (conditions: 1 mL of acetone, 4 equiv K_2CO_3 and PFP, room temperature, 5 min reaction time) compared to the selectivity observed for the combined reaction of *p*-hydroxybenzaldehyde, vanillin, and syringaldehyde. To accommodate for the high expected rate of reaction of the aldehydes in DMSO, the relative rates were measured by derivatizing the three substrates in the same vial with only 0.2 equiv of PFP based off the total phenols loaded, allowing for the selectivities of the TFP ethers to indicate the relative rates of reaction. Conditions: 1 mL of DMSO, 4 equiv of K_2CO_3, 5 min, conversion is limited by adding 0.2 equiv of PFP. (C) Yield of TFP ether for guaiacyl-type model compounds. Conditions: 5 min reaction time, 1 mL of acetone, 4 equiv of PFP and K_2CO_3. (D) Reaction of syringol in DMSO (red), acetone (yellow), and dioxane (purple). Conditions: 4 mL of solvent, 4 equiv of K_2CO_3 and PFP, room temperature. The error bars indicate the range of duplicate measurements.

When attempting to derivatize a wider array of model compounds in acetone, solubility issues were encountered. For example, when the derivatization of syringaldehyde was attempted in acetone, no product was observed in the ^{19}F NMR spectrum, and instead a white precipitate was formed. While acetone is a common laboratory solvent and allowed for the convenient measurement of the reaction rate, other solvents such as DMSO offer improved ability to dissolve a wide range of lignins.[38−40] Repeating the derivatization of syringaldehyde in DMSO showed full conversion to the TFP ether within 1 h. Aside from affecting the solubility of the substrate, solvent choice can also modulate reaction kinetics, especially for S_NAr reactions.[41,42] Given the fast reaction of vanillin, reactions were instead performed with syringol to measure the effect of solvent on the reaction rate. When DMSO was used as the solvent, full conversion of syringol to the desired TFP ether was observed within 1 min, much shorter than the 2 h required for the same reaction in acetone (Figure 2D). Reactions in dioxane, another common solvent for lignin, displayed the lowest reaction rate, achieving less than 15% conversion in 1 h. The observed solvent effect may be a result of the higher solubility of K_2CO_3 in DMSO compared to the other solvents[43,44] and reinforces the conclusion that reactivity of alcohols with PFP is dependent on the deprotonation of the alcohol. In the scope of the prescribed method, the drastic increase of the reaction rate can reduce time needed for derivatization and ultimately lead to a higher throughput if desired. We thus selected DMSO as the preferred solvent for further investigation due to the faster reaction rate and improved dissolution ability.

Given the promising results showing complete and selective conversion of model compounds to their corresponding TFP ethers, we further expanded the scope of model compounds tested to 31 total (Table S1). While quantitative yields of the desired TFP ether were observed for most model compounds using DMSO as a solvent, issues were encountered when carboxylic acid-containing models were used. For example, when syringic acid was derivatized in DMSO, only an ∼62% yield of the TFP-ether product(s) was measured across multiple resonances in the ^{19}F NMR spectrum (Figure 3A,B). Furthermore, 64% of the initial PFP loaded was converted to tetrafluorohydroxypyridine (TFHP), identified by previously reported ^{19}F NMR shifts;[45] the ^{19}F NMR resonances for TFHP do not overlap with the TFP-ether products (Figure 3B). Brittain and Cobb showed that carboxylic acids react with PFP to form acyl fluorides and TFHP. These acyl fluorides could then react further with phenols to yield esters (Figure 3C).[45] These side reactions consume the K_2CO_3 and PFP reagents and also prevent phenols from being measured, potentially precluding the method from use on substrates that contain carboxylic acids.

The acyl fluoride-forming reaction relies on the nucleophilic attack of the fluoride ion on a TFP-ester intermediate. Halides such as F^- are particularly reactive in polar aprotic solvents such as DMSO, but reactivity is reduced in protic solvents such as water.[46] Thus, we examined the impact of water content in the derivatization solvent. As water content in the derivatization solvent was increased to 20 and 40%, the yield and selectivity to a single TFP-ether resonance increased (Figure 3A,B). When the solvent contained 40% water, nearly full recovery of the desired TFP ether was observed from a single

https://doi.org/10.1021/acssuschemeng.3c00115
ACS Sustainable Chem. Eng. 2023, 11, 5644−5655

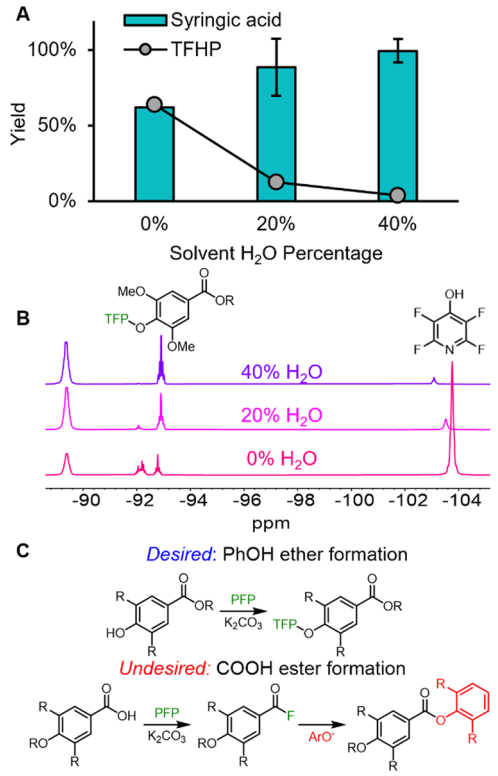

Figure 3. (A) Yield of the syringic acid-TFP ether (teal bars) and TFHP (gray circles) as a function of water content in the derivatization solvent. (B) ^{19}F NMR spectra of reactions from panel A. (C) Desired TFP-ether formation reaction from carboxylic acid-containing substrates and undesired ester production through acyl fluoride formation followed by esterification with an additional phenolic molecule. Conditions: 1 mL of reaction solvent (0, 20, or 40% H_2O/DMSO), 4 equiv of PFP and K_2CO_3, 5 min reaction time, room temperature, 2 mL of acetone added to the reaction vial to resolubilize products and internal standard; the error bars represent the range of duplicate measurements.

resonance, showing that the addition of water can prevent this side reaction (Figure 3). TFHP could form from the reaction of water and PFP; however, only 4% PFP was converted to TFHP for reactions in 40% H_2O/DMSO, indicating that TFHP is formed mainly from the acyl fluoride-forming reaction, rather than from the direct reaction of PFP and water. The presence of water in the reaction solvent is expected to increase the rate of phenolic derivatization due to the increased solubility of K_2CO_3, but the reaction occurs too quickly to confidently measure the change in rate directly.

Utilizing 40% H_2O/DMSO solvent, full conversion of the starting material was observed in 5 min for almost all phenolic monomer model compounds tested, and the average and range of observed resonances are shown in Figure 4 for each substitution pattern (the ^{19}F NMR spectra of derivatized model compounds are shown in Figures S15−S47). The one exception is that when the model compound 5-5 GG (3,3′-dimethoxy-5,5′-dipropyl[1,1′-biphenyl]-2,2′-diol), which contains two phenolic groups, was derivatized for a standard reaction time of 5 min, two resonances were observed in the ^{19}F NMR spectrum at −94.12 and −92.78 ppm (Figure S2). As the reaction time increased, the UF resonance decreased and the DF resonance increased, indicating that the DF peak is likely due to the partially derivatized product (mono-TFP ether). For a reaction time of 5 min, the mono- and di-TFP ether accounted for 59 and 25% yield of the starting material, respectively. Allowing the reaction to proceed to 3 h showed full conversion to the fully derivatized product (Figure S2B). When *ortho*-eugenol, another 5-substituted model compound, was tested, full conversion to the desired TFP ether was measured in the desired time of 5 min. These results suggest that the low quantification for 5-5 GG derives at least in part from steric blocking of the first derivatized phenol. Importantly, the partially derivatized 5-5 compound can be detected by its resonance at −94.12 ppm, which is outside of the phenolic integration range, allowing for monitoring of this issue in lignin substrates. Catechol and protocatechuic acid were both fully converted to the desired di-TFP ethers, indicating that the 1,2-dihydroxy substitution does not inhibit full derivatization. However, the derivatization of gallic acid and 3,4,5-trihydroxybenzaldehyde was unsuccessful, leading to precipitate formation and under quantification (gallic acid, 78 ± 6%; 3,4,5-trihydroxybenzaldehyde, 58 ± 2%, duplicate measurements) across multiple resonances in the ^{19}F spectrum, presumably arising from the incomplete derivatization products (Figure S3). The trihydroxy substitution pattern is known to prompt degradation reactions in the presence of oxygen, especially under alkaline conditions.[47]

Distinction between syringyl (S), guaiacyl (G), *p*-hydroxyphenyl (H), and condensed-G (G_c, G-type compounds with substitutions at the 5-position other than a methoxy group) phenolics could be achieved in both regions for most model compounds tested (Figure 4). One exception was that aldehydes such as vanillin and syringaldehyde displayed resonances that were substantially downfield of similarly substituted phenols, causing an overlap with other integrations in the DF region (Figure S4). For G_c compounds such as *ortho*-eugenol and 5-5 GG, resonances were mostly downfield of S phenolics in the UF region, indicating that G_c and S phenolics can be distinguished in this region. In the DF region, however, G_c phenols completely overlapped with the syringyl peak, indicating that this region may be a mixed measure of total 5-substituted phenols, rather than purely S-type (Figure 4, dark blue; Figure S4). Catechol and protocatechuic acid displayed DF resonances that overlapped with the H region (−91.0 ppm), but the UF resonances (−156.99 and −156.87 ppm) did not overlap with any other studied model compounds (Figure S3). Although this may indicate the possibility of using this region to quantify catechols, this region is currently included in the G region. Overall, these results indicate that PFP derivatization in 40% H_2O/DMSO followed by ^{19}F NMR allows for reasonably accurate identification of H, G, G_c, and S phenolics. The full list of shifts of all model compounds tested can be found in Table S1, and comparison of the select spectra can be seen in Figures S3, S4, and S5. Recommended integration ranges for quantifying different phenolics are given in Table S2.

Derivatization Selectivity to Phenolic Hydroxyl Groups. In addition to phenols, native and derivatized lignins contain additional hydroxyl groups at the α- and γ-positions of linkages between aromatic rings. For the PFP-based method to be effective, reactions with these alcohols must not interfere with phenolic regions in the NMR spectra. If their resonances do not overlap, their reaction can be ignored. However, if aliphatic hydroxyl resonances fall within the phenolic integration region, their reaction rate must be sufficiently slow compared to the phenolic derivatization rate to ensure high selectivity to phenolic hydroxyl groups. Aliphatic alcohols,

https://doi.org/10.1021/acssuschemeng.3c00115
ACS Sustainable Chem. Eng. 2023, 11, 5644−5655

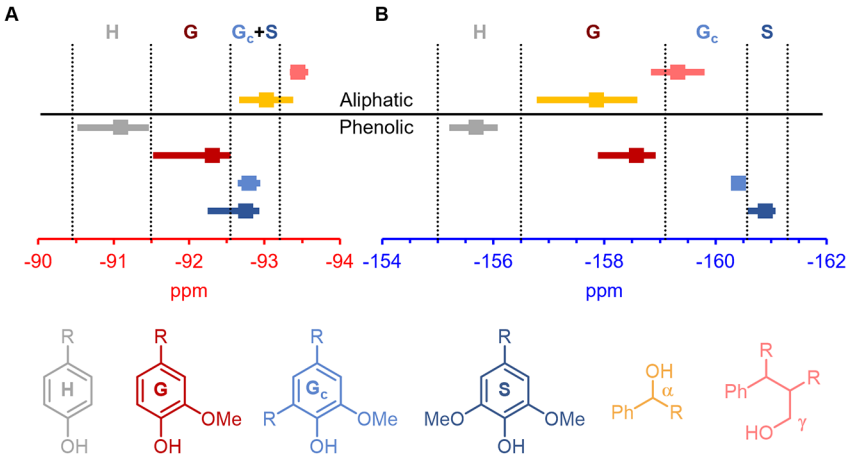

Figure 4. ^{19}F resonances of model compounds for (A) DF (−90 to −94 ppm, red axis) and (B) UF (−155 to −162 ppm, blue axis) regions for derivatizations conducted in 40% H_2O/DMSO. The square marker indicates the average shift of the models tested, and the colored lines indicate the total range observed. The vertical dotted lines show the used integration ranges. R groups tested include H, propyl, aldehydes, and carboxylic acids, among others. The number of compounds reported for each group is G_c = 2; S = 5; G = 11; H = 6; α = 7; γ = 4. Conditions: 1 mL of 40% H_2O/DMSO, 4 equiv of PFP and K_2CO_3, 5 min reaction time, room temperature, 2 mL of acetone added to the reaction vial to resolubilize products and internal standard.

especially those that lack heteroatoms such as halides, are considerably less acidic than phenolic alcohols, with aliphatic alcohols exhibiting pK_a values in the range of 15−16.[48,49] Given the evidence above that suggests the link between the pK_a value of a phenol and its TFP-ether formation rate, reactions with aliphatic alcohols were expected to be much slower than phenolic reactions. Nonetheless, acidity does not constitute the full picture of S_NAr reactivity, which also depends on the nucleophilicity of the conjugate alkoxide.

To measure the potential impact of aliphatic hydroxyl groups on the quantification of phenols, model compounds containing aliphatic hydroxyl groups were derivatized to determine their resonance and reaction rate (Table S1). Aliphatic hydroxyl groups behaved similarly to phenols, exhibiting a single resonance due to TFP-ether formation. All tested aliphatic alcohols showed resonances in the UF guaiacyl or condensed-G phenolic integration region, indicating that these alcohols would cause interference in measurements of lignins if converted to TFP ethers during derivatization. However, in the DF region, most aliphatic shifts were UF of the phenolic resonances (Figure 4, the gold markers represent the α-hydroxyl groups; the pink markers represent the γ-hydroxyl groups). The exceptions were some benzylic alcohols such as vanillyl alcohol, in which the derivatized aliphatic overlapped with the region for S phenolic hydroxyls in the DF region. For example, 3,4-dimethoxybenzyl alcohol exhibited resonances of −93.38 and −158.59 ppm, which are outside of the phenolic DF region (−90.5 to −93.2 ppm) but overlap with the UF phenolic region (−155 to −161.35 ppm). However, vanillyl alcohol displayed resonances of −93.0 and 158.44 ppm, which overlap with the DF and UF integration regions, respectively (Figure S5).

The fact that aliphatic alcohol resonances overlap with phenols to a lesser degree in the DF region compared to the UF region can give insight into the extent of aliphatic reaction during a derivatization. In the event of aliphatic reaction, additional resonances will then present in the ^{19}F NMR spectrum. In the DF region, most of these are expected to be UF of the phenolic integration region, although some will lie in the S region, which will inflate the value obtained for the phenolic content. In the UF region, all reacted aliphatics will be quantified as phenols, increasing the value obtained for the phenolic content, such that the UF measurement will be greater than the DF measurement. This difference can indicate the extent to which aliphatic alcohols have reacted, serving as an internal reference as to whether aliphatic alcohol groups are interfering in the measurement. If similar values are obtained for both regions, the interference from aliphatic hydroxyls is expected to be low, and the UF integration region should be used as the preferred region, given the greater separation between resonances. However, if the UF region quantifies a higher phenolic value than the DF region, we recommend that the DF region be used for quantification. The syringyl integral from the UF region may still be integrated since no aliphatic alcohols displayed resonances there (Figure 4).

Overall, the yields from reactions with other aliphatic alcohols show that the reaction rate, and therefore the expected potential interference with phenolic measurements, was highly dependent on the substrate (Figure 5A). Non-phenolic model compounds such as 2-(3,4-dimethoxyphenyl)-ethanol showed the highest reaction rates, achieving 51% yield to the corresponding TFP ether in 5 min in 40% H_2O/DMSO (Figure 5A). Conversely, the phenolic analogue homovanillyl alcohol exhibited only 5% conversion of the aliphatic alcohol. For the phenolic substrates vanillyl alcohol, homovanillyl alcohol, and 4-propanolguaiacol, the aliphatic yield decreased with a longer chain length. The difference in the reactivity of phenolic/nonphenolic models could be due to inherent differences in the reactivity of the respective aliphatic alcohols, such as the aliphatic alcohol of the nonphenolic models being systematically more acidic or nucleophilic than phenolic analogues, although this is not expected. Alternatively, this could indicate an effect where the presence of the phenol impacts the rate of derivatization through another mechanism, such as consumption of limited reactants. To elucidate the role of phenols on the rate of aliphatic reaction, 2-(3,4-dimethoxyphenyl)-ethanol was derivatized again, this time with a 1:1 mole ratio of 4-propylguaiacol. Only a 16% yield of the derivatized aliphatic alcohol was measured, indicating that the presence of phenols reduces the rate of aliphatic

https://doi.org/10.1021/acssuschemeng.3c00115
ACS Sustainable Chem. Eng. 2023, 11, 5644−5655

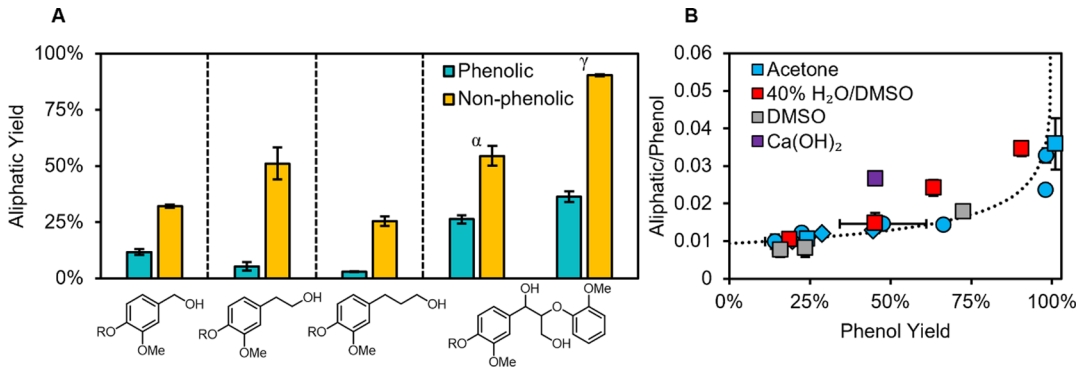

Figure 5. (A) Yield of TFP-ether products from aliphatic alcohols for phenolic (teal) and nonphenolic model compounds (yellow). Conditions: 20 mg of the substrate, 4 equiv of K_2CO_3 and PFP, 1 mL of 40% H_2O/DMSO, room temperature, 5 min reaction time, 2 mL of acetone added post reaction for resolubilization. (B) Impact of different solvent systems on the selectivity of aliphatic derivatization as a function of phenolic conversion using vanillyl alcohol as a substrate. The squares represent the partial conversion experiments, wherein conversion was controlled by limiting the PFP used. The circles correspond to the time course reactions where samples were taken consecutively from the same reaction over time with 4 equiv of PFP and K_2CO_3, whereas the diamonds represent the reactions with only 1 equiv of PFP and K_2CO_3. Conditions: 20 mg of vanillyl alcohol, 4 equiv of K_2CO_3 and PFP, unless otherwise stated, 1 mL of solvent, 2 mL of acetone added post reaction for resolubilization for reactions in 40% H_2O/DMSO. The error bars represent the range of two replicate experiments.

derivatization (Figure S6). Substrates containing the *β*-O-4 linkage such as guaiacylglycerol-*β*-guaiacyl ether (GGE) and 1-(3,4-dimethoxyphenyl)-2-(2-methoxyphenoxy)propane-1,3-diol (VGE) exhibited high reactivity compared to similarly substituted compounds (Figure 5A and Figures S7 and S8). For instance, the secondary benzylic hydroxyl group on 4-hydroxy-3-methoxy-*α*-methylbenzyl alcohol showed only 2.3% conversion to the corresponding TFP ether in 40% H_2O/DMSO after 5 min, whereas VGE showed almost 58% yield under the same conditions. The low yields of aliphatic derivatization for model compounds containing phenolic hydroxyl groups demonstrate that aliphatic interference should be low for most lignin samples that contain free phenolic groups. However, native-like lignins that contain abundant *β*-O-4 linkages may be especially prone to aliphatic interference.

To further investigate whether derivatization conditions could impact selectivity, reactions were conducted with vanillyl alcohol, which contains both a phenolic and an aliphatic alcohol group. Time course reactions in acetone showed that the benzylic alcohol was derivatized concurrently with the phenolic group, and the initial rate of phenolic derivatization was about 100 times faster than the corresponding reaction with the benzylic alcohol. When the aliphatic hydroxyl group was derivatized, the corresponding phenol resonance on the same molecule was shifted slightly downfield (Figure S9B). Complete conversion of vanillyl alcohol to the phenol-TFP derivative was observed in approximately 2 h, at which point the yield of the aliphatic TFP ether was 4% (Figure 5B, blue circles; Figure S9A). Decreasing the amount of PFP and K_2CO_3 used to 1 equiv decreased the reaction rate but did not alter the selectivity of phenol reaction over aliphatic reaction (Figure 5B, blue diamonds). Similar experiments were conducted in DMSO and 40% H_2O/DMSO, except that the conversion of the phenol was controlled by reducing the equivalents of PFP, due to the much faster rate of reaction. Changing the base from K_2CO_3 to NaOH resulted in multiple resonances, potentially from reactions at positions other than the 4-position of PFP. Using $Ca(OH)_2$, which is much less soluble in water, resulted in only 1 resonance but had a slightly lower selectivity to the phenol (Figure 5B, purple square). Regardless of the solvent and the varying overall rates of reaction, the extent of aliphatic reaction at a given phenol conversion was similar, although reactions in 40% H_2O/DMSO showed a slightly lower selectivity to phenolics. This suggests that the selectivity cannot not be appreciably modulated through solvent or base selection and that aliphatic interference can mainly be controlled by selecting the proper reaction time for the given solvent.

Application and Benchmarking of the ^{19}F NMR Method on Lignin Substrates. Given promising results of the model compound studies, we next sought to validate the ^{19}F method by comparing phenolic measurements of diverse lignin substrates to measurements obtained using ^{31}P NMR spectroscopy (Table S4) and validating the trends observed in model compound reactions.[21,50] From model compound experiments, none of the tested solvent systems showed a substantial advantage in selectivity to phenolics as a function of conversion. For the method to be useful for lignin substrates, a set reaction time should be implemented that ensures the complete derivatization of phenolic hydroxyls while minimizing the interference from aliphatic hydroxyls. The real selectivity will then depend on the absolute rates of reaction and the total time the substrate is in contact with the reagents, including the time during reaction preparation and post-reaction sampling, which is about 1 min for each sample. For reactions in acetone that occur on the order of hours, small deviations in the total reaction time for different samples are inconsequential. However, for reactions in 40% H_2O/DMSO where the TFP-ether formation is much faster, the time required for preparation and sampling is comparable to the total reaction time. Allowing reactions to proceed for slightly longer could be expected to give lower selectivity to phenols given the drastically different absolute rates of reactions. Thus, it is important to confirm the insensitivity of phenolic selectivity on the derivatization solvent.

We first investigated PFP derivatization of reductive catalytic fractionation oil (RCF oil) from poplar in acetone. While acetone showed a lower reaction rate and dissolution ability compared to DMSO for experiments with model compounds, its use also allowed for the measurement of spectral characteristics and quantifications as a function of time, providing confirmation of trends seen in model compound

https://doi.org/10.1021/acssuschemeng.3c00115
ACS Sustainable Chem. Eng. 2023, 11, 5644−5655

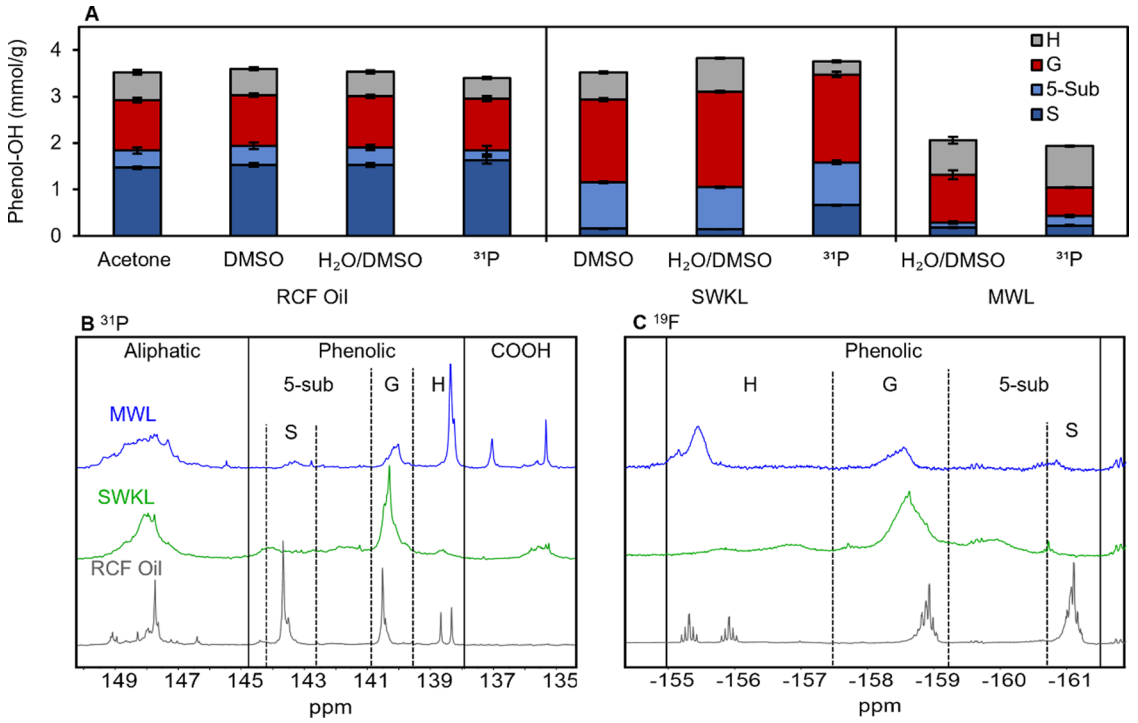

Figure 6. (A) Comparison of various ^{19}F derivatizations with ^{31}P NMR results. (B) ^{31}P spectra of tested lignins. (C) ^{19}F spectra of tested lignins. Reactions conducted in 10 mL glass vials at room temperature using 20−40 mg of the lignin substrate, 4 equiv of PFP and K_2CO_3 for DMSO and 40% H_2O/DMSO reactions and 2 equiv for acetone reactions, reaction time of 24 h for acetone, 1 h for DMSO, and 5 min for 40% H_2O/DMSO. For reactions in 40% H_2O/DMSO, 2 mL of acetone was added to resolubilize the precipitated lignin. The error bars show the standard deviation of three replicate measurements. See Figure 7 for the statistical comparison of the ^{31}P NMR method with the ^{19}F NMR using 40% H_2O/DMSO.

experiments. The RCF process cleaves β-O-4 ether bonds in lignin, leading to a highly depolymerized oil with phenolic monomers, as well as dimers and oligomers containing carbon−carbon linkages.[51,52] While RCF oil is still a complex mixture, a high percentage of its constituent molecules are aromatic monomers that are routinely quantified, making it comparatively simpler than native lignin.[53,54] Approximately 200 mg of RCF oil was derivatized in a 10 mL vial with 10 mL of acetone with 2 equiv of PFP and K_2CO_3 using a small stir bar (see the SI for the impact of the stir bar size), and samples were time obtained by filtering an aliquot of each vial at the desired reaction time. Within 1 h of reaction time, well-resolved peaks for S and G moieties expected of a hardwood began to appear (Figure S10A). Poplar also contains *p*-hydroxybenzoate (PHBA) pendent units that are ester-linked to lignin and cell wall components.[55,56] PHBA is converted to methyl paraben and phenol during RCF in methanol,[57] and these can be individually resolved in both the ^{19}F and ^{31}P methods (Figure 6B and Figure S10A). As expected from model compound studies, these H units reacted the fastest, followed by G and then S species (Figure S10B,C).

Comparison of the DF and UF regions showed that the quantifications of H and total phenol were indistinguishable at each time point. However, there was disagreement between the S- and G-type quantifications (Figure S10D). Notably, the quantity of total 5-substituted phenolics quantified from the DF region was lower than that obtained from the UF region (DF, 1.55 ± 0.01; UF, 1.84 ± 0.07; ^{31}P, 1.85 ± 0.09 mmol/g) and more closely reflected the measure of purely S-type phenols measured from the UF region (UF, 1.47 ± 0.03; ^{31}P, 1.63 ± 0.07 mmol/g). This was compensated by the DF region quantifying a higher number of G-type phenols than the UF region (DF, 1.36 ± 0.02; UF, 1.09 ± 0.05; ^{31}P, 1.11 ± 0.05 mmol/g). This discrepancy may derive from species that are quantified as 5-substituted in the UF region but as G in the DF region. Model compound studies showed that aldehyde-substituted compounds, such as syringaldehyde, were substantially downfield of other S model compounds tested; however, the presence of oxidized substituents is unlikely, given the reducing reaction conditions of RCF. Alternatively, RCF oil could contain additional G_c compounds whose resonances fall downfield of the tested G_c model compounds, 5-5 GG and *o*-eugenol, and the DF resonances may overlap with G phenolics in the DF regions. Nonetheless, the identical total quantifications between the UF and DF regions show that aliphatic hydroxyl groups were not interfering to a large extent, and thus the UF region can be confidently used for quantification. After 24 h of reaction, the quantification of total phenolics in the UF region showed no statistically significant differences to the values obtained using the ^{31}P NMR-based method (Figure 6A; ^{19}F, 3.52 ± 0.1; ^{31}P, 3.40 ± 0.2; α = 0.05). Allowing the reaction to proceed for 48 h led to little change in integration values or spectral characteristics, confirming that the reaction with the aliphatic hydroxyl groups is slow. Further leaving the reaction for 6 days eventually led to the appearance of additional resonances and increased integration values, presumably from the eventual reaction of aliphatic hydroxyl groups.

To confirm the solvent effects observed during model compound experiments, derivatization of RCF oil was repeated in pure DMSO (1 h reaction time) and 40% H_2O/DMSO (5 min reaction time) using large stir bars. As expected, the reaction proceeded much faster in the more polar solvents. When the 40% H_2O/DMSO system was used, the lignin began

https://doi.org/10.1021/acssuschemeng.3c00115
ACS Sustainable Chem. Eng. 2023, 11, 5644−5655

to precipitate shortly after the addition of PFP, necessitating the addition of solvent for resolubilization after 5 min of reaction time. By using the ratio of 1 mL reaction volume to 2 mL of acetone, we observed full resolubilization of the lignin sample and internal standard. Identical quantifications were obtained for all measurements compared regardless of the solvent (α = 0.05), indicating that phenol selectivity remained the same at the time of measurement despite the differences in the absolute reaction rate (DMSO UF, 3.59 ± 0.1 mmol/g; 40% H_2O/DMSO UF, 3.52 ± 0.1; Figure 6A and Figure S11). The similar quantifications obtained when using pure DMSO and 40% H_2O/DMSO as solvents can be attributed to the lack of carboxylic acids in the RCF oil as measured by the ^{31}P method. Similar to reactions in acetone, allowing reactions in DMSO and 40% H_2O/DMSO to proceed for additional time led to the quantification increasing above the value measured from the ^{31}P method, presumably from the formation of aliphatic TFP ethers. This increase with continued reaction time was more pronounced in the UF region than the DF region, in line with the observation that most aliphatic hydroxyl group shifts do not overlap the DF region.

We next tested the derivatization of softwood kraft lignin (SWKL) with DMSO and 40% H_2O/DMSO solvents, since SWKL is not soluble in acetone. The kraft process consists of hydrothermal treatment of wood in the presence of NaOH and Na_2S, inducing extensive structural changes to the lignin.[58,59] These conditions prompt the formation of recalcitrant C−C bonds at the expense of aryl-ether linkages. Much work has gone into elucidating the resultant structure, but it is still largely uncertain.[58,59] When SWKL was derivatized in DMSO, a slightly lower than expected phenolic quantification (^{19}F UF, 3.52 ± 0.08 mmol/g; ^{31}P, 3.77 ± 0.07 mmol/g) was obtained (Figure 6A). This is possibly due to the presence of carboxylic acids (0.62 ± 0.02 mmol/g as measured by the ^{31}P method), leading to esterification and depletion of phenols. Repeating this derivatization in 40% H_2O/DMSO for 5 min led to a higher quantification of 3.92 ± 0.05 mmol/g (Figure 6A). DF quantification was only slightly lower at 3.71 ± 0.07 mmol/g total phenols. Extending the derivatization time to 10 min did not alter the quantification, indicating that phenols are fully derivatized within the 5 min reaction time (Figure S12). Identification of structural motifs between the ^{19}F and ^{31}P methods was significantly different: ^{31}P NMR measured 0.67 ± 0.01 mmol/g of syringyl phenolics; however, lignin derived from softwoods should only contain guaiacyl and *p*-hydroxyphenyl moieties.[60] This is a known problem with ^{31}P NMR spectroscopy deriving from the significant overlap between G_c and S phenolics, regardless of the ^{31}P derivatization agent used.[11] The ^{19}F method measures 0.15 ± 0.01 mmol/g of syringyl units in the UF region, potentially showing that this method has less overlap between S and condensed-G phenolics. Total 5-substituted content from the ^{19}F method was still under-quantified relative to ^{31}P NMR (UF ^{19}F, 1.05 ± 0.01; ^{31}P, 1.59 ± 0.02), and the corresponding measurements of G and H units were higher. This may be due to the presence of nonconventional lignin phenols such as substituted catechols, but it is uncertain which method gives a better description of the functional groups, given the lesser-known structure of the lignin.

The method was applied to corn stover MWL. MWL is intended to represent native lignin,[61] and ^{31}P NMR shows that there are a greater number of aliphatic alcohols (2.90 ± 0.03 mmol/g) than phenolics (1.94 ± 0.05 mmol/g) as expected from a lignin that has not been extensively depolymerized (Table S4). When the ^{19}F method was applied, the UF integration region measurement was 20% higher (2.48 ± 0.07 mmol/g) than the DF region (2.06 ± 0.2 mmol/g) (Figure S13). This is likely due to aliphatic reaction during derivatization, and thus only the DF region was used for integration. From model compound experiments with GGE and VGE, it is expected that β-O-4 structures in the MWL caused the increased aliphatic reaction compared to the RCF oil and SWKL. Reasonable assignment of the phenol type was achieved, with ^{19}F measuring a higher amount of G-type phenols (DF ^{19}F, 1.02 ± 0.09; ^{31}P, 0.61 ± 0.01) at the expense of 5-substituted (DF ^{19}F, 0.29 ± 0.02; ^{31}P, 0.43 ± 0.02) and H-type (DF ^{19}F, 0.75 ± 0.07; ^{31}P, 0.89 ± 0.01) phenolics.

We thought that mixing could be especially important for reactions in 40% H_2O/DMSO due to the precipitation of the derivatized lignin during the reaction. Interestingly, using a medium stir bar led to a slightly lower quantification than values obtained using the large stir bar for all three substrates, although results were only significantly different for SWKL (Figure S1). We thus recommend the use of a large stir bar.

For any quantitative measurement, sample stability is an important consideration. Sample degradation may prevent accurate quantification and limits analytical throughput and flexibility. Sample stability was measured for each solvent system where applicable by leaving the samples in the NMR tubes at room temperature. In the DMSO-based systems, performing ^{19}F NMR experiments on derivatized RCF oil up to 14 days after derivatization resulted in identical integrations compared to the samples analyzed immediately after derivatization, implying that they are stable (Figure S11C). However, the measured phenolic content of samples derivatized in 40% H_2O/DMSO increased by 3−6% over the course of 24 h (Figure S14A), indicating that these samples should be analyzed immediately for best results. It is worth noting that ^{31}P samples are known to begin degrading immediately depending on the sample and internal standard, and it is also recommended that samples are analyzed immediately.[11,27] Experiments with SWKL conducted with two internal standards (4,4-difluorobenzophenone and 1,4-difluoro-2,5-dimethoxybenzene) showed no deviation in their expected ratio, nor did their relative integrations change over the course of 48 h (Figure S14B). The increase in the measured phenolic content therefore appears to be caused by the continued reaction with aliphatic alcohols enabled perhaps by the increased solubility of K_2CO_3 with the addition of water, rather than degradation of the internal standard, as is common with the ^{31}P method.

Overall, the ^{19}F-based method appears to agree well with the results obtained from ^{31}P NMR spectroscopy, with all R^2 values greater than 0.9 (Figure 7A). To assess the agreement of the ^{19}F method compared to the ^{31}P method more thoroughly, *t*-tests were performed on quantifications of total phenolics and individual species (Figure 7B). Total phenolics are very closely recovered; however, SWKL is significantly different ($p \leq 0.05$). RCF oil is quantified most closely, with only the value of H phenolics qualifying as statistically significantly different (DF ^{19}F, 0.52 ± 0.03; ^{31}P, 0.44 ± 0.03). However, almost all individual quantifications for SWKL and MWL are significantly different, which indicates that the two methods are not equivalent for these more structurally complex lignins. While minimal deviations in the resonance classifications were observed for model compounds, these differences may point

https://doi.org/10.1021/acssuschemeng.3c00115
ACS Sustainable Chem. Eng. 2023, 11, 5644−5655

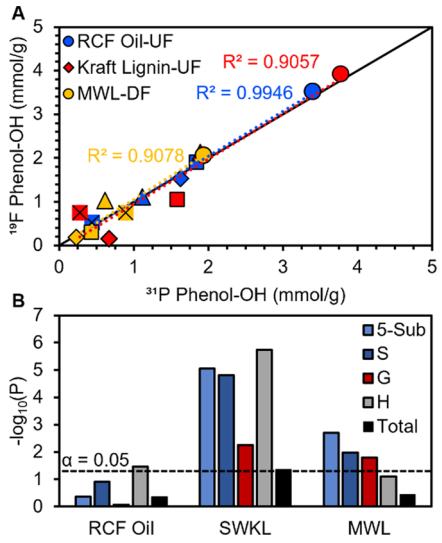

Figure 7. (A) Parity plot of quantifications of total phenol (circle), total 5-substituted (square), S (diamond), G (triangle), and H (square with cross) obtained from the ^{31}P NMR method and the ^{19}F NMR method using 40% H_2O/DMSO as the solvent. (B) Negative logarithm of the *p*-value obtained from comparing ^{31}P and ^{19}F NMR measurements.

to unexamined species in the SWKL and MWL, which violate the classifications, and a more in-depth structural characterization is needed to determine the origin of these differences.

CONCLUSIONS

In summary, we developed a phenolic measurement method using PFP as a derivatizing agent followed by ^{19}F NMR spectroscopy. Reactions with aliphatic alcohol groups can be limited by tuning the reaction time. If carboxylic acids are not expected to be present, such as in lignins without ester-linked units, pure DMSO can be used as a solvent (1 h reaction time), and samples can be assumed stable. In such cases, the ^{19}F method could be amenable to high-throughput analysis. The presence of carboxylic acids necessitates the use of 40% water as a co-solvent with a shorter derivatization reaction time of 5 min, and samples should be analyzed immediately. The method achieved comparable results to ^{31}P NMR spectroscopy in terms of total phenolic measurement for the three diverse lignins studied. Similar distributions of functional groups were obtained for corn stover MWL and poplar RCF oil, but SWKL showed significantly different results; most notably, 5-substituted groups were under-quantified using the PFP-based method. The ^{19}F method exhibits advantages in both the low cost of the derivatization reagent and its low toxicity, but it does not overcome the issue of sample stability that is present in the ^{31}P NMR method. Furthermore, the ^{19}F method is hindered by both aliphatic alcohols and carboxylic acids, whereas the ^{31}P method efficiently measures all hydroxyl groups. Further developments of this approach could focus on evaluating derivatization conditions to minimize the interference of aliphatic alcohols, but nonetheless, the method can find immediate application to supplement the analytical toolbox available to lignin chemists.

ASSOCIATED CONTENT

Supporting Information

The Supporting Information is available free of charge at https://pubs.acs.org/doi/10.1021/acssuschemeng.3c00115.

Model compound shifts, additional model compound reaction figures, lignin substrate time course reactions in various solvents, and ^{19}F NMR spectra of all model compounds in 40% H_2O/DMSO (Figures S15−S47) (PDF)

AUTHOR INFORMATION

Corresponding Author

Gregg T. Beckham − *Department of Chemical and Biological Engineering, University of Colorado Boulder, Boulder 80303 Colorado, United States; Renewable Resources and Enabling Sciences Center, National Renewable Energy Laboratory, Golden, Colorado 80401, United States;* orcid.org/0000-0002-3480-212X; Email: gregg.beckham@nrel.gov

Authors

Jacob K. Kenny − *Department of Chemical and Biological Engineering, University of Colorado Boulder, Boulder 80303 Colorado, United States; Renewable Resources and Enabling Sciences Center, National Renewable Energy Laboratory, Golden, Colorado 80401, United States*

J. Will Medlin − *Department of Chemical and Biological Engineering, University of Colorado Boulder, Boulder 80303 Colorado, United States*

Complete contact information is available at: https://pubs.acs.org/10.1021/acssuschemeng.3c00115

Author Contributions

The manuscript was written through contributions of all authors. All authors have given approval to the final version of the manuscript.

Funding

This work was authored by the Alliance for Sustainable Energy, LLC, the manager and operator of the National Renewable Energy Laboratory for the U.S. Department of Energy (DOE), under contract no. DE-AC36-08GO28308. J.K.K., J.W.M., and G.T.B. were funded by The Center for Bioenergy Innovation, a U.S. DOE Bioenergy Research Center supported by the Office of Biological and Environmental Research in the DOE Office of Science. G.T.B. also thanks the U.S. Department of Energy Office of Energy Efficiency and Renewable Energy Bioenergy Technologies Office for funding. The views expressed herein do not necessarily represent the views of the DOE or the U.S. Government. The U.S. Government retains and the publisher, by accepting the article for publication, acknowledges that the U.S. Government retains a non-exclusive, paid-up, irrevocable, worldwide license to publish or reproduce the published form of this work, or allow others to do so, for U.S. Government purposes.

Notes

The authors declare no competing financial interest.

ACKNOWLEDGMENTS

We thank Liz Ware and Renee Happs for help with the ^{31}P NMR measurements and Ciaran Lahive and Mikhail Konev for helpful discussions and a critical reading of the manuscript. We thank Reagan Dreiling for help with production of the

reductive catalytic fractionation oil. We also thank Rui Katahira for providing the 5-5 GG model compound, 4-propylsyringol model compound, and corn stover milled wood lignin.

■ ABBREVIATIONS

NMR, nuclear magnetic resonance; PFP, pentafluoropyridine; TMDP, 2-chloro-4,4,5,5-tetramethyl-1,3,2-dioxaphospholane; H, *para*-hydroxyphenyl; G, guaiacyl; S, syringyl; G_c, guaiacyl-condensed; TFP, tetrafluoropyridyl; GHS, Globally Harmonized System of Classification and Labelling of Chemicals; T_1, spin−lattice relaxation parameter; RCF, reductive catalytic fractionation; SWKL, softwood kraft lignin; MWL, milled wood lignin; UF, upfield; DF, downfield; DMSO, dimethyl sulfoxide; TFHP, tetrafluorohydroxypyridine; GGE, guaiacylglycerol-*β*-guaiacyl ether; VGE, 1-(3,4-dimethoxyphenyl)-2-(2-methoxyphenoxy)propane-1,3-diol

■ REFERENCES

(1) Boerjan, W.; Ralph, J.; Baucher, M. Lignin Biosynthesis. *Annu. Rev. Plant Biol.* **2003**, *54*, 519−546.
(2) del Río, J. C.; Rencoret, J.; Gutierrez, A.; Elder, T.; Kim, H.; Ralph, J. Lignin Monomers from beyond the Canonical Monolignol Biosynthetic Pathway − Another Brick in the Wall. *ACS Sustainable Chem. Eng.* **2020**, *8*, 4997−5012.
(3) Schutyser, W.; Renders, T.; Van Den Bosch, S.; Koelewijn, S. F.; Beckham, G. T.; Sels, B. F. Chemicals from Lignin: An Interplay of Lignocellulose Fractionation, Depolymerisation, and Upgrading. *Chem. Soc. Rev.* **2018**, *47*, 852−908.
(4) Bartling, A. W.; Stone, M. L.; Hanes, R. J.; Bhatt, A.; Zhang, Y.; Biddy, M. J.; Davis, R.; Kruger, J. S.; Thornburg, N. E.; Luterbacher, J. S.; Rinaldi, R.; Samec, J. S. M.; Sels, B. F.; Román-Leshkov, Y.; Beckham, G. T. Techno-Economic Analysis and Life Cycle Assessment of a Biorefinery Utilizing Reductive Catalytic Fractionation. *Energy Environ. Sci.* **2021**, *14*, 4147−4168.
(5) Corona, A.; Biddy, M. J.; Vardon, D. R.; Birkved, M.; Hauschild, M. Z.; Beckham, G. T. Life Cycle Assessment of Adipic Acid Production from Lignin. *Green Chem.* **2018**, *20*, 3857−3866.
(6) Davis, R.; Tao, L.; Tan, E. C. D.; Biddy, M. J.; Beckham, G. T.; Scarlata, C.; Jacobson, J.; Cafferty, K.; Ross, J.; Lukas, J.; Knorr, D.; Schoen, P. *Process Design and Economics for the Conversion of Lignocellulosic Biomass to Hydrocarbons: Dilute-Acid and Enzymatic Deconstruction of Biomass to Sugars and Biological Conversion of Sugars to Hydrocarbons*; National Renewable Energy Lab 2013. DOI: 10.2172/1176746.
(7) Huang, K.; Fasahati, P.; Maravelias, C. T. System-Level Analysis of Lignin Valorization in Lignocellulosic Biorefineries. *iScience* **2020**, *23*, 100751.
(8) Rinaldi, R.; Jastrzebski, R.; Clough, M. T.; Ralph, J.; Kennema, M.; Bruijnincx, P. C. A.; Weckhuysen, B. M. Paving the Way for Lignin Valorisation: Recent Advances in Bioengineering, Biorefining and Catalysis. *Angew. Chem., Int. Ed.* **2016**, *55*, 8164−8215.
(9) Laurichesse, S.; Avérous, L. Chemical Modification of Lignins: Towards Biobased Polymers. *Prog. Polym. Sci.* **2014**, 1266−1290.
(10) Duval, A.; Lawoko, M. Reactive & Functional Polymers A Review on Lignin-Based Polymeric, Micro- and Nano-Structured Materials. *React. Funct. Polym.* **2014**, *85*, 78−96.
(11) Balakshin, M.; Capanema, E. On the Quantification of Lignin Hydroxyl Groups with ^{31}P and ^{13}C NMR Spectroscopy. *J. Wood Chem. Technol.* **2015**, *35*, 220−237.
(12) Jääskeläinen, A. S.; Sun, Y.; Argyropoulos, D. S.; Tamminen, T.; Hortling, B. The Effect of Isolation Method on the Chemical Structure of Residual Lignin. *Wood Sci. Technol.* **2003**, *37*, 91−102.
(13) Lin, Y. S.; Dence, W. C. *Methods in Lignin Chemistry*; 1992, DOI: 10.1007/978-3-642-74065-7.
(14) Faix, O.; Argyropoulos, D. S.; Robert, D.; Neirinck, V. Determination of Hydroxyl Groups in Lignins Evaluation of ^{1}H- ^{13}C-, ^{31}P-NMR. FTIR and Wet Chemical Methods. *Holzforschung* **1994**, *48*, 387−394.
(15) Barrelle, M. A New Method for the Quantitative 19F NMR Spectroscopic Analysis of Hydroxyl Groups in Lignins. *Holzforschung* **1993**, *47*, 261−267.
(16) Barrelle, M. Improvements in the Structural Investigation of Lignins by ^{19}F NMR Spectroscopy. *J. Wood Chem. Technol.* **1995**, *15*, 179−188.
(17) Esakkimuthu, E. S.; Marlin, N.; Brochier-Salon, M.-C.; Mortha, G. Study of the Reactivity of Lignin Model Compounds to Fluorobenzylation Using 13C and 19F NMR. *Molecules* **2020**, *25*, 3211.
(18) Capanema, E. A.; Balakshin, M. Y.; Kadla, J. F. Quantitative Characterization of a Hardwood Milled Wood Lignin by Nuclear Magnetic Resonance Spectroscopy. *J. Agric. Food Chem.* **2005**, *53*, 9639−9649.
(19) Capanema, E. A.; Balakshin, M. Y.; Kadla, J. F. A Comprehensive Approach for Quantitative Lignin Characterization by NMR Spectroscopy. *J. Agric. Food Chem.* **2004**, *52*, 1850−1860.
(20) Mansfield, S. D.; Kim, H.; Lu, F.; Ralph, J. Whole Plant Cell Wall Characterization Using Solution-State 2D NMR. *Nat. Protoc.* **2012**, *7*, 1579−1589.
(21) Meng, X.; Crestini, C.; Ben, H.; Hao, N.; Pu, Y.; Ragauskas, A. J.; Argyropoulos, D. S. Determination of Hydroxyl Groups in Biorefinery Resources via Quantitative ^{31}P NMR Spectroscopy. *Nat. Protoc.* **2019**, *14*, 2627−2647.
(22) Schiff, D. E.; Verkade, J. G.; Metzler, R. M.; Squires, T. G.; Venier, C. G. Determination of Alcohols, Phenols, and Carboxylic Acids Using Phosphorus-31 Nmr Spectroscopy. *Appl. Spectrosc.* **1986**, *40*, 348−351.
(23) Lensink, C.; Markuszewski, R.; Verkade, J. G.; Wroblewski, A. E. ^{31}P NMR Spectroscopic Analysis of Coal Pyrolysis Condensates and Extracts for Heteroatom Functionalities Possessing Labile Hydrogen. *Energy Fuels* **1988**, *2*, 765−774.
(24) Argyropoulos, D. S. Quantitative Phosphorus-31 Nmr Analysis of Lignins, a New Tool for the Lignin Chemist. *J. Wood Chem. Technol.* **1994**, *14*, 45−63.
(25) Archipov, Y.; Argyropoulos, D. S.; Bolker, H. I.; Heitner, C. ^{31}P NMR Spectroscopy in Wood Chemistry. I. Model Compounds. *J. Wood Chem. Technol.* **1991**, *11*, 137−157.
(26) Argyropoulos, D. S.; Bolker, H. I.; Heitner, C.; Archipov, Y. ^{31}P NMR Spectroscopy in Wood Chemistry. Part V. Qualitative Analysis of Lignin Functional Groups. *J. Wood Chem. Technol.* **1993**, *13*, 187−212.
(27) Ben, H.; Ferrell, J. R. In-Depth Investigation on Quantitative Characterization of Pyrolysis Oil by ^{31}P NMR. *RSC Adv.* **2016**, *6*, 17567−17573.
(28) Brittain, W. D. G.; Cobb, S. L. Tetrafluoropyridyl (TFP): A General Phenol Protecting Group Readily Cleaved under Mild Conditions. *Org. Biomol. Chem.* **2019**, *17*, 2110−2115.
(29) Brandner, D. G.; Kruger, J. S.; Thornburg, N. E.; Facas, G. G.; Kenny, J. K.; Dreiling, R. J.; Morais, A. R. C.; Renders, T.; Cleveland, N. S.; Happs, R. M.; Katahira, R.; Vinzant, T. B.; Wilcox, D. G.; Román-Leshkov, Y.; Beckham, G. T. Flow-through Solvolysis Enables Production of Native-like Lignin from Biomass. *Green Chem.* **2021**, *23*, 5437−5441.
(30) Dong, X.; Mayes, H. B.; Morreel, K.; Katahira, R.; Li, Y.; Ralph, J.; Black, B. A.; Beckham, G. T. Energy-Resolved Mass Spectrometry as a Tool for Identification of Lignin Depolymerization Products. *ChemSusChem* **2023**, e202201441.
(31) Meng, X.; Pu, Y.; Yoo, C. G.; Li, M.; Bali, G.; Park, D. Y.; Gjersing, E.; Davis, M. F.; Muchero, W.; Tuskan, G. A.; Tschaplinski, T. J.; Ragauskas, A. J. An In-Depth Understanding of Biomass Recalcitrance Using Natural Poplar Variants as the Feedstock. *ChemSusChem* **2017**, *10*, 139−150.
(32) Kojima, M.; Tsunoi, S.; Tanaka, M. Determination of 4-Alkylphenols by Novel Derivatization and Gas Chromatography-Mass Spectrometry. *J. Chromatogr. A* **2003**, *984*, 237−243.

(33) Fuhrer, T. J.; Houck, M.; Corley, C. A.; Iacono, S. T. Theoretical Explanation of Reaction Site Selectivity in the Addition of a Phenoxy Group to Perfluoropyridine. *J. Phys. Chem. A* **2019**, *123*, 9450−9455.
(34) Li, X.; Russell, R. K. Using Potassium Carbonate to Scavenge Hydrogen Fluoride: A Scale-up Process for Quantitative Production of (1-Cyclopropyl-6,7-Difluoro-1,4-Dihydro-8- Methoxy-4-(0x0-K0)-3-Quinolinecarboxylato-K03)Difluoro Boron. *Org. Process Res. Dev.* **2008**, *12*, 464−466.
(35) Ragnar, M.; Lindgren, C. T.; Nilvebrant, N.-O. PKa-Values of Guaiacyl and Syringyl Phenols Related to Lignin. *J. Wood Chem. Technol.* **2000**, *20*, 277−305.
(36) Ralph, J.; Lundquist, K.; Brunow, G.; Lu, F.; Kim, H.; Schatz, P. F.; Marita, J. M.; Hatfield, R. D.; Ralph, S. A.; Christensen, J. H.; Boerjan, W. Lignins: Natural Polymers from Oxidative Coupling of 4-Hydroxyphenyl- Propanoids. *Phytochem. Rev.* **2004**, *3*, 29−60.
(37) Ahvazi, B. C.; Crestini, C.; Argyropoulos, D. S. ^{19}F Nuclear Magnetic Resonance Spectroscopy for the Quantitative Detection and Classification of Carbonyl Groups in Lignins. *J. Agric. Food Chem.* **1999**, *47*, 190−201.
(38) Sameni, J.; Krigstin, S.; Sain, M. Solubility of Lignin and Acetylated Lignin in Organic Solvents. *BioResources* **2016**, *12*, 1548−1565.
(39) Duval, A.; Vilaplana, F.; Crestini, C.; Lawoko, M. Solvent Screening for the Fractionation of Industrial Kraft Lignin. *Holzforschung* **2016**, *70*, 11−20.
(40) Dastpak, A.; Lourençon, T. V.; Balakshin, M.; Farhan Hashmi, S.; Lundström, M.; Wilson, B. P. Solubility Study of Lignin in Industrial Organic Solvents and Investigation of Electrochemical Properties of Spray-Coated Solutions. *Ind. Crops Prod.* **2020**, *2020*, 148.
(41) Miguel, E. L. M.; Santos, C. I. L.; Silva, C. M.; Pliego, J. R. How Accurate Is the SMD Model for Predicting Free Energy Barriers for Nucleophilic Substitution Reactions in Polar Protic and Dipolar Aprotic Solvents? *J. Braz. Chem. Soc.* **2016**, *27*, 2055−2061.
(42) Pliego, J. R.; Piló-Veloso, D. Effects of Ion-Pairing and Hydration on the SNAr Reaction of the F- with p-Chlorobenzonitrile in Aprotic Solvents. *Phys. Chem. Chem. Phys.* **2008**, *10*, 1118−1124.
(43) Li, M.; Constantinescu, D.; Wang, L.; Mohs, A.; Gmehling, J. Solubilities of NaCl, KCl, LiCl, and LiBr in Methanol, Ethanol, Acetone, and Mixed Solvents and Correlation Using the Liquac Model. *Ind. Eng. Chem. Res.* **2010**, *49*, 4981−4988.
(44) Long, B. Experimental Studies and Thermodynamic Modeling of the Solubilities of Potassium Nitrate, Potassium Chloride, Potassium Bromide, and Sodium Chloride in Dimethyl Sulfoxide. *Ind. Eng. Chem. Res.* **2011**, *50*, 7019−7026.
(45) Brittain, W. D. G.; Cobb, S. L. Carboxylic Acid Deoxyfluorination and One-Pot Amide Bond Formation Using Pentafluoropyridine (PFP). *Org. Lett.* **2021**, *23*, 5793−5798.
(46) Vlasov, V. M. Fluoride Ion as a Nucleophile and a Leaving Group in Aromatic Nucleophilic Substitution Reactions. *J. Fluorine Chem.* **1993**, *61*, 193−216.
(47) Honda, S.; Ishida, R.; Hidaka, K.; Masuda, T. Stability of Polyphenols under Alkaline Conditions and the Formation of a Xanthine Oxidase Inhibitor from Gallic Acid in a Solution at PH 7.4. *Food Sci. Technol. Res.* **2019**, *25*, 123−129.
(48) Jinhua, Z.; Kleinöder, T.; Gasteiger, J. Prediction of PKa Values for Aliphatic Carboxylic Acids and Alcohols with Empirical Atomic Charge Descriptors. *J. Chem. Inf. Model.* **2006**, *46*, 2256−2266.
(49) Cabrera, Y.; Cabrera, A.; Jensen, A.; Felby, C. Purification of Biorefinery Lignin with Alcohols. *J. Wood Chem. Technol.* **2016**, *36*, 339−352.
(50) Granata, A.; Argyropoulos, D. S. 2-Chloro-4,4,5,5-Tetramethyl-1,3,2-Dioxaphospholane, a Reagent for the Accurate Determination of the Uncondensed and Condensed Phenolic Moieties in Lignins. *J. Agric. Food Chem.* **1995**, *43*, 1538−1544.
(51) Schutyser, W.; Kruger, J. S.; Robinson, A. M.; Katahira, R.; Brandner, D. G.; Cleveland, N. S.; Mittal, A.; Peterson, D. J.; Meilan, R.; Román-leshkov, Y.; Beckham, G. T. Revisiting Alkaline Aerobic Lignin Oxidation. *Green Chem.* **2018**, 3828−3844.
(52) Abu-Omar, M. M.; Barta, K.; Beckham, G. T.; Luterbacher, J. S.; Ralph, J.; Rinaldi, R.; Román-Leshkov, Y.; Samec, J. S. M.; Sels, B. F.; Wang, F. Guidelines for Performing Lignin-First Biorefining. *Energy Environ. Sci.* **2021**, *14*, 262−292.
(53) Anderson, E. M.; Michael, L.; Katahira, R.; Beckham, G. T.; Anderson, E. M.; Stone, M. L.; Katahira, R.; Reed, M.; Beckham, G. T.; Román-Leshkov, Y. Flowthrough Reductive Catalytic Fractionation of Biomass Flowthrough Reductive Catalytic Fractionation of Biomass. *Joule* **2017**, *1*, 613−622.
(54) Dao Thi, H.; Van Aelst, K.; Van den Bosch, S.; Katahira, R.; Beckham, G. T.; Sels, B. F.; Van Geem, K. M. Identification and Quantification of Lignin Monomers and Oligomers from Reductive Catalytic Fractionation of Pine Wood with GC × GC − FID/MS. *Green Chem.* **2022**, 191.
(55) Mottiar, Y.; Karlen, S. D.; Goacher, R. E.; Ralph, J.; Mansfield, S. D. Metabolic Engineering of P-Hydroxybenzoate in Poplar Lignin. *Plant Biotechnol. J.* **2023**, 1−188.
(56) Goacher, R. E.; Mottiar, Y.; Mansfield, S. D. ToF-SIMS Imaging Reveals That p-Hydroxybenzoate Groups Specifically Decorate the Lignin of Fibres in the Xylem of Poplar and Willow. *Holzforschung* **2021**, *75*, 452−462.
(57) Kenny, J. K.; Brandner, D. G.; Neefe, S. R.; Michener, W. E.; Román-leshkov, Y.; Beckham, G. T.; Medlin, J. W. Catalyst Choice Impacts Aromatic Monomer Yields and Selectivity in Hydrogen-Free Reductive Catalytic Fractionation. *React. Chem. Eng.* **2022**, 2527.
(58) Crestini, C.; Lange, H.; Sette, M.; Argyropoulos, D. S. On the Structure of Softwood Kraft Lignin. *Green Chem.* **2017**, *19*, 4104−4121.
(59) Lancefield, C. S.; Wienk, H. J. L.; Boelens, R.; Weckhuysen, B. M.; Bruijnincx, P. C. A. Identification of a Diagnostic Structural Motif Reveals a New Reaction Intermediate and Condensation Pathway in Kraft Lignin Formation. *Chem. Sci.* **2018**, *9*, 6348−6360.
(60) Vanholme, R.; Demedts, B.; Morreel, K.; Ralph, J.; Boerjan, W. Lignin Biosynthesis and Structure. *Plant Physiol.* **2010**, *153*, 895−905.
(61) Balakshin, M.; Capanema, E. A.; Zhu, X.; Sulaeva, I.; Potthast, A.; Rosenau, T.; Rojas, O. J. Spruce Milled Wood Lignin: Linear, Branched or Cross-Linked? *Green Chem.* **2020**, *22*, 3985−4001.

https://doi.org/10.1021/acssuschemeng.3c00115
ACS Sustainable Chem. Eng. 2023, 11, 5644−5655